Structural and enzymatic characterization of NanS (YjhS), a 9-*O*-Acetyl *N*-acetylneuraminic acid esterase from *Escherichia coli O157:H7*

Erumbi S. Rangarajan,[1][†] Karen M. Ruane,[1][†] Ariane Proteau,[1] Joseph D. Schrag,[2] Ricardo Valladares,[3] Claudio F. Gonzalez,[3] Michel Gilbert,[4] Alexander F. Yakunin,[5] and Miroslaw Cygler[1,2]*

[1]Department of Biochemistry, McGill University, Montreal, Quebec, Canada

[2]Biotechnology Research Institute, Montreal, Quebec H4P 2R2, Canada

[3]Department of Microbiology and Cell Science, University of Florida, Gainesville, Florida 32610-3610

[4]Institute for Biological Sciences, National Research Council Canada, Ottawa, Ontario K1A 0R6, Canada

[5]Banting and Best Department of Medical Research, Department of Chemical Engineering and Applied Chemistry, University of Toronto, Toronto, Ontario M5G 1L6, Canada

Abstract: There is a high prevalence of sialic acid in a number of different organisms, resulting in there being a myriad of different enzymes that can exploit it as a fermentable carbon source. One such enzyme is NanS, a carbohydrate esterase that we show here deacetylates the 9 position of 9-*O*-sialic acid so that it can be readily transported into the cell for catabolism. Through structural studies, we show that NanS adopts a SGNH hydrolase fold. Although the backbone of the structure is similar to previously characterized family members, sequence comparisons indicate that this family can be further subdivided into two subfamilies with somewhat different fingerprints. NanS is the founding member of group II. Its catalytic center contains Ser19 and His301 but no Asp/Glu is present to form the classical catalytic triad. The contribution of Ser19 and His301 to catalysis was confirmed by mutagenesis. In addition to structural characterization, we have mapped the specificity of NanS using a battery of substrates.

Keywords: carbohydrate esterase; crystal structure; SGNH hydrolase; sialic acid; substrate profile

Introduction

Acetylation of carbohydrates yielding singly or multiple *O*- or *N*-acetylated forms and their subsequent deacetylation occurs commonly in nature. The multiplicity of enzymes involved in deacetylation is reflected by the classification of carbohydrate esterases within 16 groups in the carbohydrate active enzymes database, CAZy (http://www.cazy.org/;[1]). Despite its wide occurrence, in many instances, we have an incomplete understanding of the function of carbohydrate acetylation and deacetylation, as well as the enzymes involved in these processes. The deacetylase enzymes can be grouped within two broad functional classes: those that remove acetyl groups from carbohydrate units of polysaccharides, including pectin,[2] xylan,[3] galactoglucomannan,[4] chitin,[5] rhamnogalacturonan,[6] or conjugated sialic acids[7,8] as part of their catabolism of carbon sources, and those associated with a regulatory or virulence-related function, often found within pathogenic bacteria.[9–11] Many of these *N*- and *O*-deacetylases show a relatively broad substrate specificity profile with a variety of naturally occurring and synthetic substrates,[12–14] although some are remarkably specific for their natural substrate, such as the enzymes in carbohydrate esterase family (CE) 2 which are specific for the 6-*O*-deacetylation of aldohexoses.[15]

In higher organisms, sialic acid (2-keto-3-deoxy-5-acetamido-D-*glycero*-D-*galacto*-nonulosonic acid) is usually found as a glycoconjugate, which plays diverse roles in a range of biologically important processes from cell-cell recognition and signaling to neural development.[16,17] Some bacteria, in particular pathogenic strains, utilize sialic acid as a decoy molecule, where it is often found as part of the capsular polysaccharide or of lipopolysaccharide,[9] allowing the pathogen to evade the host immune response by masquerading as "self" (reviewed in Ref. 16). The abundance of sialic acid within the host, especially in the mucosal environment, provides a source of carbon and nitrogen for bacteria such as *Escherichia coli,* which possess pathways to catabolize sialic acid.[16,18] The enzymes in these pathways are coregulated in response to the sialic acid environment that surrounds the pathogen, in particular the presence of the most common form of sialic acid, *N*-acetyl neuraminic acid (Neu5Ac). In *E. coli,* there are three operons, *nanATEK-yhcH*, *nanCMS* (formerly *yjhATS*), and *yjhBC*, whose enzyme products have been shown or are predicted to be involved in a sialic acid catabolism, and whose expression is regulated by the NanR repressor in response to Neu5Ac concentration-dependent manner.[16,19]

The functions of all three enzymes within the *nanCMS* operon have been assigned. NanC (YjhA) is an outer membrane porin inducible by Neu5Ac.[20] NanM (YjhT) is a mutarotase which produces the thermodynamically more stable beta form of sialic acid from its corresponding alpha isomer.[21] NanS (YjhS) was annotated as a putative acetylxylan esterase or 9-*O*-sialic acid esterase and has recently been shown to be capable of using 9-*O*-acetyl *N*-acetyl neuraminic acid (Neu5,9Ac$_2$) as a substrate and is necessary for the ability of *E. coli* to grow on this sugar.[8] NanS is a member of a relatively small family of characterized bacterial sialate esterases, including the bi-functional synthetase/*O*-acetylesterase NeuA from group B *Streptococcus,*[22] and a related enzyme from *E. coli* K1.[23] Both enzymes show the capacity for removing acetyl groups from the 9-*O* position of sialic acid.[22,23]

Sialate esterases are found in all forms of life. For example, in mammals, the enzyme SIAE has been showed to remove the 9-*O*-acetyl group of acetylated sialic acid.[24] This processing is necessary for B cell function as the deacetylation at the 9 position is required for interaction with CD22 and possibly other Siglecs.[25] Mutations in the SIAE gene have recently been linked to autoimmunity.[26] The first viral sialate esterase to be identified was from the influenza C virus.[27] Since then, a number of sialic acid modifying esterases have been identified in corona- and toroviruses.[28] Although it is known that sialate esterases exist in prokaryotes, especially in intestinal bacteria, to our knowledge no bacterial 9-*O*-acetyl sialate esterase has been structurally characterized.

NanS is predicted to belong to the SGNH superfamily of hydrolases,[29] a distinct class from the well-characterized α/β-hydrolases.[30] This classification is based on the presence of the catalytic serine (S), the oxyanion hole forming residues glycine (G), and asparagine (N) along with an invariant histidine (H).[31] Each of these residues are located within blocks of conserved sequences present in all family members regardless of catalytic function, and they all employ a nucleophile-His-Acid catalytic triad for efficient hydrolysis of their substrates. The SGNH hydrolase scaffold contains a central, five-stranded parallel β-sheet that is flanked by α-helices on either side. The nucleophile is situated on a sharp turn between a β-strand and the leading α-helix, while the invariant histidine is situated within a loop preceding the C-terminal α-helix. The aspartate that is part of the catalytic triad is situated two residues prior to the invariant histidine. This makes SGNH hydrolases different from other hydrolases, wherein the aspartate follows the histidine in the primary sequence.

Although crystal structures are available for a number of carbohydrate acetyl esterases from a variety of sequence families,[13,32–34] little structural information is available for those enzymes that deacetylate sialic acid. Here, we report the crystal structure of NanS and characterize its enzymatic activity profile using a variety of potential substrates. Structural investigation revealed that NanS (YjhS)

has indeed an SGNH esterase fold. Only two catalytic residues, Ser19 and His301, have been identified; the closest acidic residue, Glu26, is not close enough to His301 to fulfill the role of the third member of the classic triad. Enzymatic studies showed it to be a sialate esterase that deacetylates the 9-O position of Neu5,9Ac$_2$.

Results and Discussion

NanS activity profile

In *E. coli,* the *nanS* gene is found along with *nanC* and *nanM* in the nan*CMS* operon.[35] It has been established that NanC is an *N*-acetylneuraminic acid outer membrane channel protein and the gene is regulated by NanR, which is a regulator of *N*-acetylneuraminic acid (sialic acid) metabolism in *E. coli.*[20] The other product of the operon, NanM, is a sialic acid mutarotase that has a dimeric β-propeller structure.[21]

It has been observed that the presence of *O*-acetyl substitutions at positions 4, 7, 8, or 9 on sialic acids reduces the rate of action of many, but not all, sialidases (or neuraminidases).[7] Therefore, deacetylation of sialic acid is necessary for efficient catabolism of sialic acids, as performed by the products of *nanATEK* operon, and also for the transport through outer membrane by NanC. Based on this, we speculated that NanS performs the role of deacetylating 9-*O*-acetylated sialic acid, as it is one of the most predominant forms found among the acetylated sialic acids.[36] The presence of *nanS* in the same operon as that of *nanC* pointed toward the probable involvement of NanS in *N*-acetylneuraminic acid metabolism. Recently, NanS was shown to be required for *E. coli* cells to grow in the presence of Neu5,9Ac$_2$ and was postulated to be a 9-*O*-acetyl *N*-acetylneuraminic acid esterase.[8]

We decided to investigate the enzymatic activity of NanS *in vitro* using a set of standard reaction conditions[37,38] to define its substrate specificity. Enzymatic assays showed that NanS is clearly an esterase, in agreement with our expectations and the predictions of Steenbergen *et al*.[8] These results showed that NanS is active against an array of synthetic substrates, with the highest activity being observed against acetyl-esters, especially those containing bulky groups such as phenyl acetate, in comparison with carboxyl-esters containing extended alkyl chains. NanS showed negligible aryl esterase activity with α-naphthyl acetate and α-naphthyl propionate as substrates. No measurable lipolytic activity (turbidimetric assay) or thioesterase activity was detected with various coenzyme A derivatives.

To better define the selectivity of NanS, a more detailed investigation was carried out using a battery of closely related substrates, with a larger spectrum of acetyl-containing groups tested (Fig. 1(a), Table I). Low-level activity was observed for more bulky acetylated compounds, as was predicted from the initial screen. However, the esterase activity with these synthetic substrates is over one order of magnitude less than that observed for the predicted
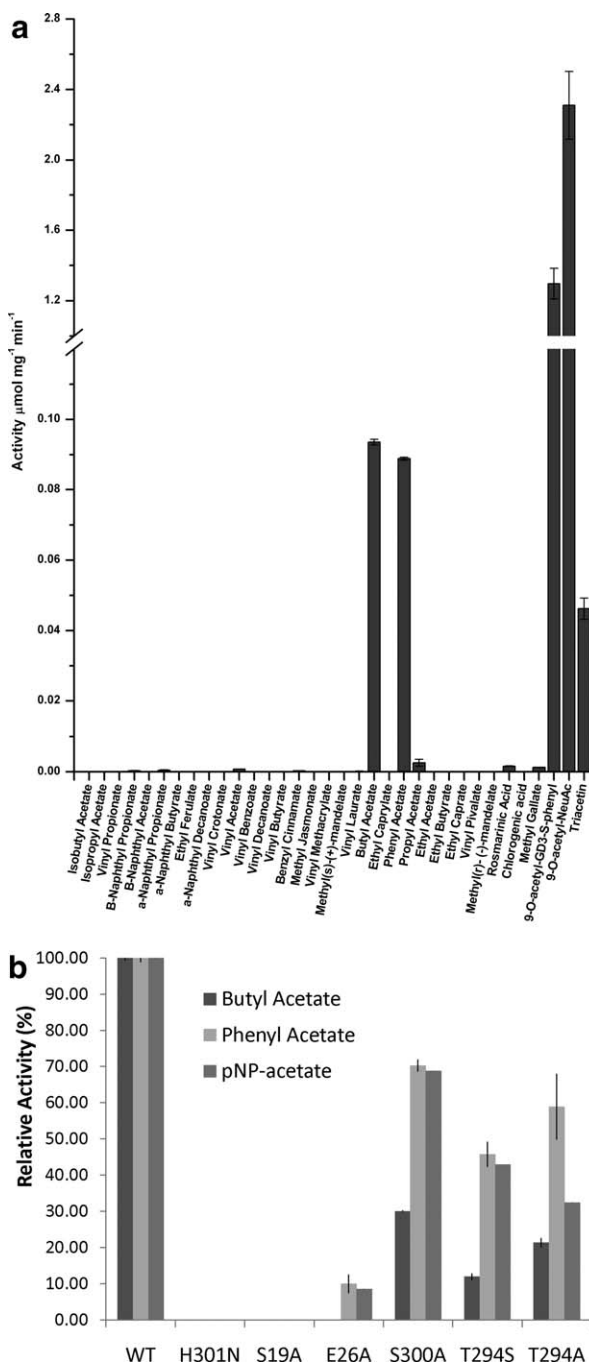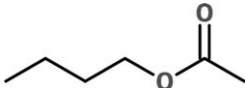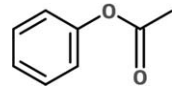
Figure 1. Esterase activity of NanS. (a) A range of substrates that were used to define the substrate selectivity profile (see also Table I); (b) Mutant activity compared to wild type NanS (see Table II). The bars on the graph indicate standard deviation. The substrates were butyl acetate, phenyl acetate and pNP-acetate. H301N and S19A show no activity while the remaining four mutants show varying levels of activity.

Table I. *Activity of NanS for Assayed Substrates that are Processed by the Enzyme*

Substrate	Activity (μmol mg^{-1} min^{-1})	Structure
Butyl acetate	0.093 ± 0.05	
Phenyl acetate	0.088 ± 0.01	
Triacetin	0.046 ± 0.04	
9-*O*-acetyl-NeuAc	2.31 ± 0.31	
9-O-acetyl-GD3-S-phenyl (9-*O*-acetyl-NeuAcα-2,8-NeuAcα-2,3-Galβ-1,4-Glcβ-*S*-phenyl)	1.29 ± 0.18	

true substrate, 9-*O*-acetyl-NeuAc (Fig. 1). This is consistent with 9-*O*-acetyl-NeuAc being the natural substrate for this enzyme.

Monomer structure

NanS exists as a monomer in solution, which was established using size exclusion chromatography as well as dynamic light scattering experiments (data not shown). This was further confirmed by the crystal structure of NanS, 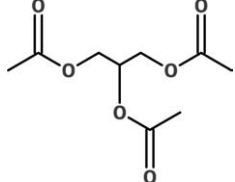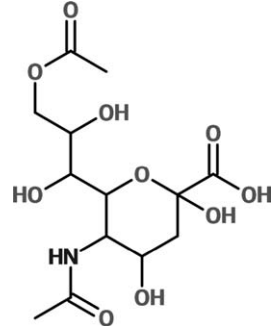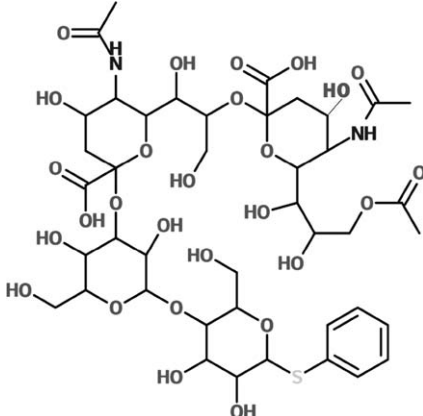which shows that NanS is a monomer. NanS consists of a single compact domain resembling a canonical α/β-hydrolase fold [Figs. 2 and 3(a)] and more specifically the SGNH family.[29] The monomer has a central seven-stranded mixed β-sheet with a strand order of β5↓β2↑β6↑β1↑β9↑ β10↑β11↑. Additionally, two β-hairpins are present following strands β2 and β6. The N- and C-terminal

α-helices, α1 and α7 respectively, are situated on the concave side of the β-sheet while the remaining α-helices (α2, α4, and α6) are positioned on the convex side with α3 and α5 being one-turn 3_{10}-helices. Several extended loops are present on the concave side of the β-sheet. One solvent exposed loop (Asn216-Thr218) located between α4 and β6 is disordered in our structure.

Structure comparisons

Proteins with the highest structural similarity to NanS determined using the DALI server[39] include the At4g34215 gene product from *Arabidopsis thaliana* (PDB ID 2APJ, *Z*-score = 25.9, rmsd 2.1 Å over 220 Cα atoms[40]), an acetyl xylan esterase related protein (AXE) from *Clostridium acetobutylicum* (PDB ID 1ZMB, *Z*-score = 24.2, rmsd 2.1 Å over 214 Cα atoms,
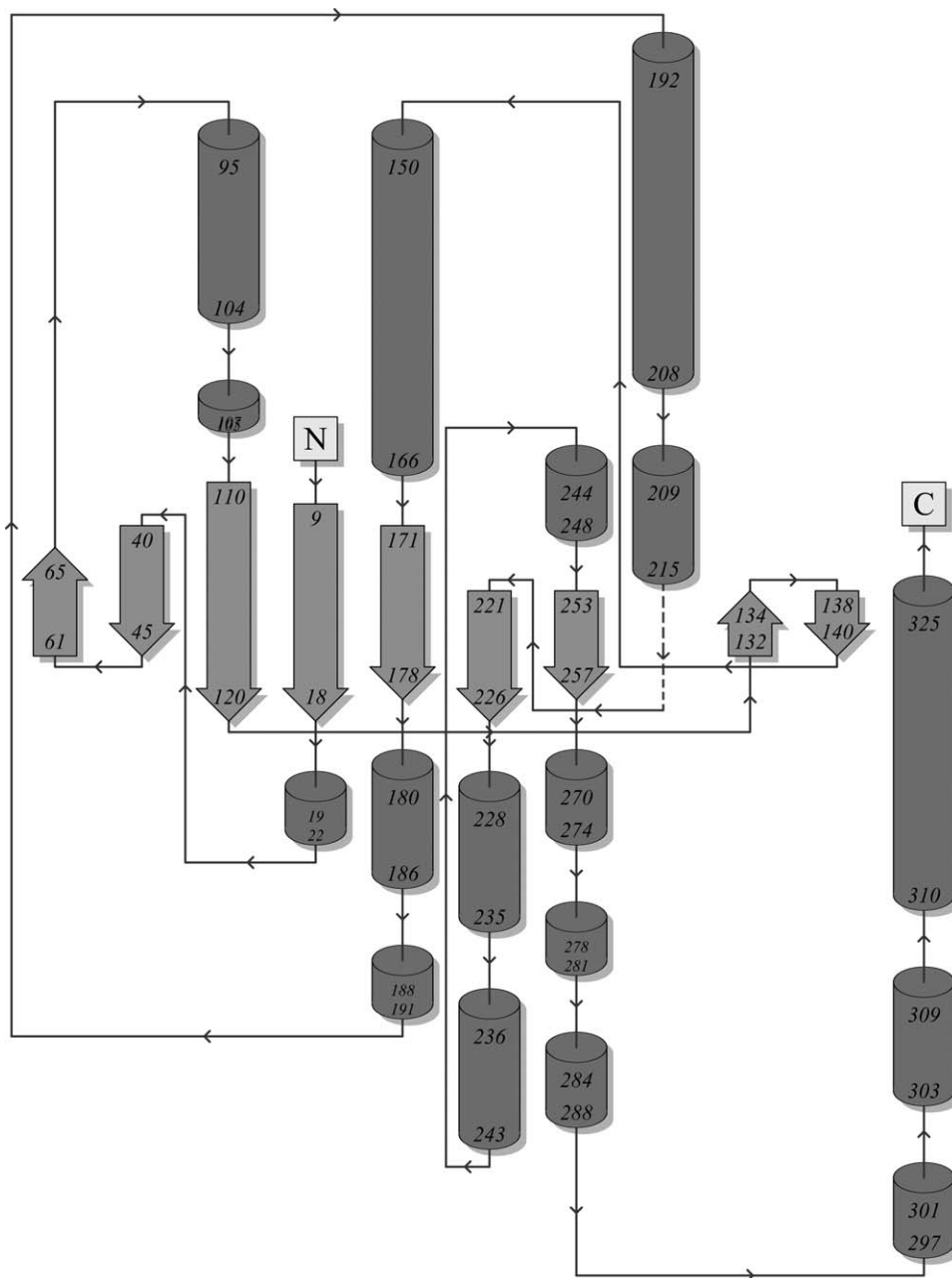
Figure 2. A topological representation of NanS. α helices are shown as cylinders, β sheets as arrows, which show their direction and random coil as lines. The short section (216–218) that was not observed in the crystal structure is shown as a dashed line. Image created using PDBSum (http://www.ebi.ac.uk/pdbsum/)

unpublished) and an acyl esterase from *Mycobacterium smegmatis* that catalyses acyl transfer to alcohols under aqueous conditions from *Mycobacterium smegmatis* (PDB ID 2Q0S, Z-score = 13.6, rmsd 2.9 Å over 179 Cα atoms[41]). All of these proteins belong to the SGNH superfamily,[29,31] with the first two proteins belong to carbohydrate esterase family 6 (CE6). The structurally characterized members of the SGNH superfamily include a serine esterase (SsEst) from *Streptomyces scabies* (PDB ID 1ESC[42]) [Fig. 3(b)], platelet activating factor acetyl-hydrolase (PAF-AH(Ib)α1) from *Bos taurus* (PDB ID 1WAB[43]), a haemagglutinin-esterase fusion (HEF) glycoprotein from influenza C

virus (PDB ID 1FLC[44]), rhamnogalacturonan acetylesterase (RGAE) from *Aspergillus aculeatus*, a CE12 member (PDB ID 1DEO[29]), and thioesterase I (TAP) from *E. coli* (PDB ID 1JRL[31]). All these enzymes have a conserved overall fold with similar relative positions of the central β-sheet and five α-helices flanking either side of the sheet as well as similar catalytic machinery, in particular serine and histidine residues. However, this similarity does not extend to their substrate binding sites. Different conformations of extended loops around the substrate binding site create distinct sites to accommodate their very different substrates [Fig. 3(b)].
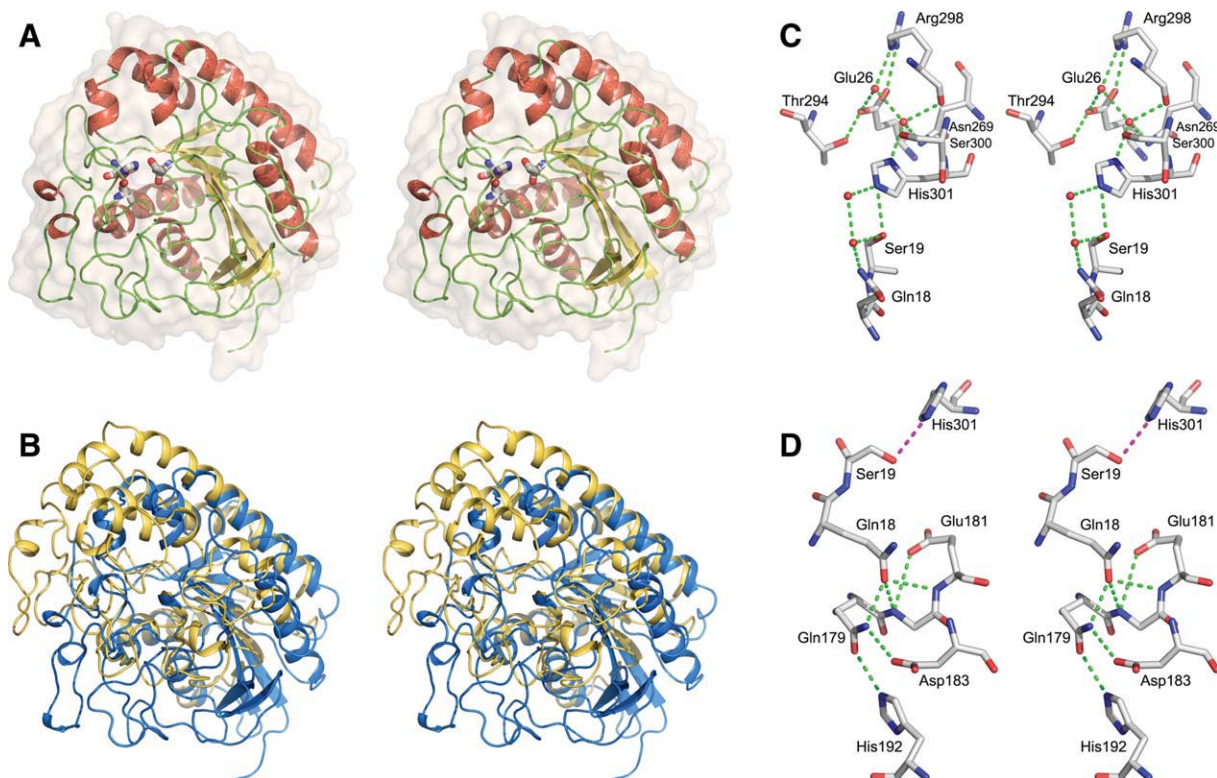
Figure 3. Structure of NanS and comparison with other SGNH enzymes. (a) Stereo view showing cartoon representation of NanS colored by secondary structure elements, Red represents α helices, yellow β sheet, and green random coil. The active site residues, His301 and Ser19, are shown in stick mode to indicate the location of the substrate binding site. Semitransparent molecular surface is colored wheat; (b) superposition of NanS (family II), shown in blue, and serine esterase SsEst (family I, PDB code 1ESC), shown in yellow. They are in the same orientation as the monomer above; (c) hydrogen bond network (green dashed lines) in the active site pocket in NanS. (d) All residues that are involved in the hydrogen bonding network of the oxyanion hole in NanS are shown. Magenta dashed line shows the interaction between the catalytic residues. This network is conserved in all family II members. For both (c) and (d), residues are shown as sticks and colored according to convention. Water molecules are shown as red spheres. All images were created using Pymol (www.pymol.org) [Color figure can be viewed in the online issue, which is available at wileyonlinelibrary.com].

Sequence motifs and two subfamilies of SGNH hydrolases

Analysis of the SGNH family of hydrolases revealed the presence of four blocks of conserved sequences.[29] Block I contains the GDS motif, which has the nucleophilic serine residue and a hydrogen-bond donor to the oxyanion hole. Block II contains the conserved Gly and block III contains the conserved Asn, which are involved in the oxyanion hole. The conserved Asn of block III encompasses the GXN motif. The final block, block IV, contains the two catalytic residues, aspartic acid and histidine, within the DXXH motif.

NanS and its structurally similar homologs AXE and the At4g34215 gene product, contain a variation in the motifs common to the SGNH family hydrolases. These differences were first noted by Bitto *et al.*[40] in the At4g34215 structure. Instead of the classic GD**S** motif of block I, these enzymes possess a more extensive GQ**S**N motif (Fig. 4). The glutamine (Gln18 in NanS) that is adjacent to the catalytic serine (Ser19 in NanS) participates as a hydrogen bond

donor in forming an oxyanion hole and functionally replaces the asparagine (part of the GXN Block III motif) found in the classic SGNH family proteins. The **G**XN block III motif is replaced by Q**G**EX(D/N). These residues are involved in stabilizing the orientation of Gln18 and a single turn 3_{10}-helix structural element. Block II is extended and now includes PCX$_2$GG instead of only the conserved Gly, which is attributed to the stabilization of the formation of the oxyanion hole. Interestingly, the Asp in block IV DXXH motif, which constitutes the third member of the catalytic triad, is not always present.

The presence of modified, conserved motifs in NanS and its close sequence homologs suggests that the SGNH hydrolase family can be further subdivided. Accordingly, we propose that sequences containing the classic serine (GDS), glycine, asparagine (GXN), and histidine in four different sequence motifs, as described earlier,[29,31] should be reclassified as group-I SGNH hydrolases, while the sequences containing serine and asparagine in a single sequence motif (GQSN) with an additional QGE
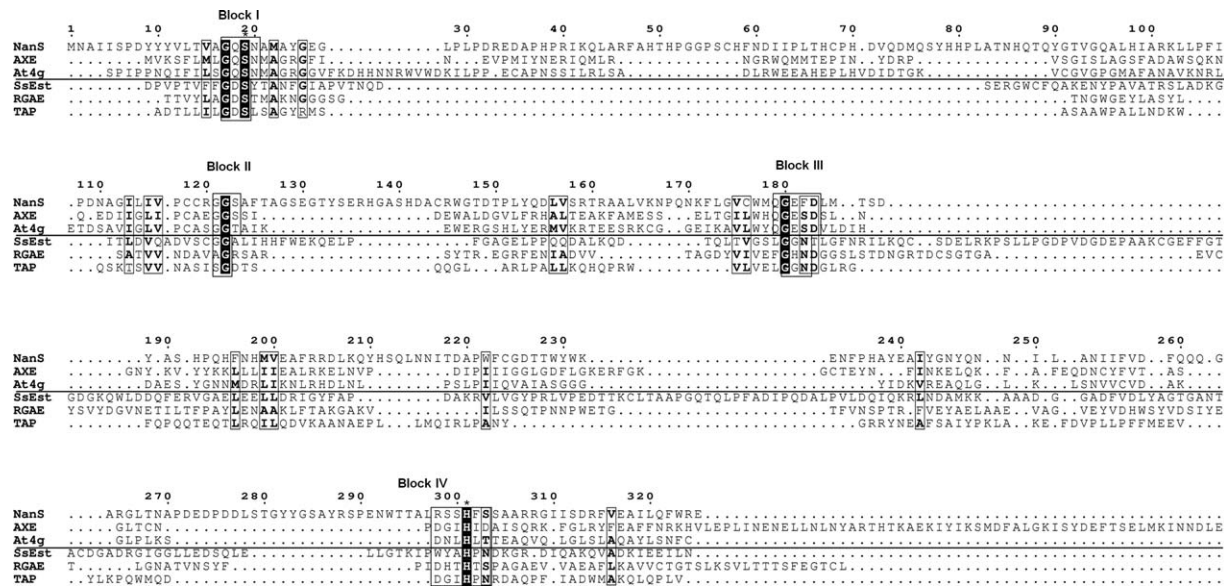
Block I

```
                    Block I
  1        10        20          30        40        50        60        70        80        90        100
NanS  MNAIISPDYYYVLTVAGQSNAMAYGEG............LPLPDREDAPHPRIKQLARFAHTHPGGPSCHFNDIIPLTHCPH.DVQDMQSYHHPLATNHQTQYGTVGQALHIARKLLPFI
AXE   .......MVKSFLMAGQSNMAYGFI.............N...EVPMIYNERIQMLR..........NGRWQMMTEPIN..YDRP...........VSGISLAGSFADAWSQKN
At4g  ........SPIPPNQIFILSGQSNMAGRGFGVFKDHHNNRWVWDKILPP.ECAPNSSILRLSA...........DLRWEEAHEPLHVDIDTGK...........VCGVGPGMAFANAVKNRL
SsEst .......DPVPTVFIGDSITANFGIAPVTNQD.................................SERGWCFQAKENYPAVATRSLADKG
RGAE  .........TTVYLAGDSTMAKNGGGSG..................................TNGWGEYLASYL..
TAP   .........ADTLLILGDSLSAGYRMS.................................ASAAWPALLNDKW....
```

```
                    Block II                                              Block III
  110       120       130       140       150       160       170       180
NanS  .PDNAGILIV.PCCRGGSAFTAGSEGTYSERHGASHDACRWGTDTPLYQDLVSRTRAALVKNPQNKFLGVCWMQGEFDLM..TSD.........
AXE   .Q.EDIIGLI.PCAEGGSSI................DEWALDGVLFRHALTEAKFAMESS...ELTGILWHQGESDSL..N..................
At4g  ETDSAVIGLV.PCASGGTAIK................EWERGSHLYERMVKRTEESRKCG..GEIKAVLWYQGESDVLDIH.................
SsEst ...ITLDVQADVSCGGALIHHFWEKQELP...........FGAGELPPQQDALKQD........TQLTVGSLGGNTLGFNRILKQC..SDELRKPSLLPGDPVDGDEPAAKCGEFFGT
RGAE  .....SATVV.NDAVAGRSAR...............SYTR.EGRFENIADVV..........TAGDYVIVEFGHNDGGSLSTDNGRTDCSGTGA.....................EVC
TAP   ...QSKTSVV.NASISGDTS...............QQGL...ARLPALLKQHQPRW.......VLVELGGNDGLRG...................
```

```
  190       200       210       220       230       240       250       260
NanS  ........Y.AS.HPQHFNHMVEAFRRDLKQYHSQLNNITDAPWFCGDITWYWK.........................ENFPHAYEAIYGNYQN..N..I.L..ANIIFVD..FQQQ.G
AXE   ......GNY.KV.YYKKLLLIIEALRKELNVP........DIPIIIGGLGDFLGKERFGK...........GCTEYN...FINKELQK..F..A.FEQDNCYFVT..AS....
At4g  .......DAES.YGNNMDRLIKNLRHDLNL.........PSLPIIQVAIASGGG............YIDKVREAQLG..L..K...LSNVVCVD..AK....
SsEst GDGKQWLDDQFERVGAELEELLDRIGYFAP.........DAKRVLVGYPRLVPEDTTKCLTAAPGQTQLPFADIPQDALPVLDQIQKRLNDAMKK..AAAD.G..GADFVDLYAGTGANT
RGAE  YSVYDGVNETILTFPAYLENAAKLFTAKGAKV.........ILSSQTPNNPWETG...........TFVNSPTR.FVEYAELAAE..VAG..VEYVDHWSYVDSIYE
TAP   .......FQPQQTEQTLRQILQDVKAANAEPL..LMQIRLPANY.......................GRRYNEAFSAIYPKLA..KE.FDVPLLPFFMEEV....
```

```
                    Block IV
  270       280       290       300       310       320
NanS  ....ARGLTNAPDEDPDDLSTGYYGSAYRSPENWTTAIRSSFFSSAARRGIISDRFVEAILQFWRE...
AXE   .....GLTCN...................PDGILIDAISQRK.FGLRYFEAFFNRKHVLEPLINENELLNLNYARTHTKAEKIYIKSMDFALGKISYDEFTSELMKINNDLE
At4g  .....GLPLKS..............DNLLLTTEAQVQ.LGLSLAQAYLSNFC.....
SsEst ACDGADRGIGGLLEDSQLE...........LLGTKIBWYAHPNDKGR.DIQAKQVADKIEEILN...
RGAE  T......LGNATVNSYF...............PIDHTGTSPAGAEV.VAEAFLKAVVCTGTSLKSVLTTTSFEGTCL...
TAP   ..YLKPQWMQD.................DGIHPNRDAQPF.IADWMAKQLQPLV....
```

Figure 4. Structure-based sequence alignment of several enzymes from Family I and Family II SGNH hydrolases. Representing Family II, which are shown above the line, are NanS, acetyl xylan esterase (AXE) from *Clostridium acetobutylicum* (PDB ID 2APJ) and the At4g34215 gene product (At4g) from *Arabidopsis thaliana* (PDB ID 1ZMB). The sequences that represent Family I, below the line, are serine esterase (SsEst) from *Streptomyces scabies* (PDB ID 1ESC), rhamnogalacturonan acetylesterase (RGAE) from *Aspergillus aculeatus*, (PDB ID 1DEO) and thioesterase I (TAP) from *E. coli* (PDB ID 1JRL). Each conserved Block is labeled. White letter in a black box indicate residues that are conserved in all sequences. Bold boxed letters indicate conserved residue types in some of the sequences.

sequence motif in block III, should be classified as group-II SGNH hydrolases.

The difference in sequence conservation between NanS and Group-I SGNH hydrolases results in different hydrogen-bonding interactions within the active site. These interactions seem to be specific for Group-II proteins. The hydrogen bonding interactions involved in oxyanion hole formation in the active site of NanS revealed that $OE1^{Gln18}$ is stabilized by hydrogen bonds with $NE2^{Gln179}$, N^{Gly180}, and N^{Glu181} [Fig. 3(c,d)]. Additionally, the orientation of Gln179 is stabilized further through $NE2^{Gln17}$ to $OD2^{Asp183}$ and $OE1^{Gln17}$ to $NE2^{His192}$ hydrogen bonds. In most related sequences, His192 is replaced by a tyrosine, which could also participate in similar hydrogen bonding interactions with $OE1^{Gln179}$. Similar hydrogen bonding interactions would be expected in all structures belonging to the Group-II SGNH family as the structure-based sequence alignment of Group-II SGNH hydrolases shows conservation of residues involved in this network.

The proposed classification is consistent with structural differences between these two groups. Group-I proteins, represented by the crystal structures of PAF-AH(Ib)α1, SsEst, RGAE, and HEF, posses a central, five stranded parallel β-sheet, while in the members of Group-II, represented by NanS, AXE, and the At4g34215 esterase, this β-sheet is extended by two strands at one end, with the last strand being antiparallel to the rest. The insertion found between the N-terminal β-strand and the fol-

lowing α-helix is significantly longer in Group-II members (∼70 residues in NanS) as compared to ∼30–40 residues in Group-I members.

NanS has not yet been classified within a specific carbohydrate esterase family in the CAZy database. Our sequence comparisons show that it is related to family CE6, which also contains AXE and At4g34215. Although other prokaryotic 9-*O*-sialate esterases have been identified[22,23] and have been predicted to adopt the SGNH hydrolase fold,[23] sequence conservation shows that they would belong to Group-I SGNH hydrolases. However, the mammalian sialate esterase SIAE that has been predicted to be a SGNH hydrolase, does contain the Group-II sequence motifs.

Active site and catalysis

The putative substrate-binding site in NanS, as deduced from the crystal structure and loss in activity of mutant enzymes, consists of a solvent-exposed shallow pocket [Fig. 3(a,c)]. The active site cavity is not as well defined as in some other esterases of the SGNH family such as At4g34215 gene product from *A. thaliana,*[40] SsEst from *S. scabies*[42] and AXE from *C. acetobutylicum* (PDB ID 1ZMB). However, the size of this pocket is comparable with those seen in PAF-AH(Ib)α1 and influenza C virus HEF. The shallow active site is consistent with the binding of both monomeric, acetylated sialic acid substrates and polymeric substrates such as acetyl xylan.

Table II. *Relative Activity of the Mutant Enzymes Measured for Three Substrates Compared with the Wild Type NanS*

Substrate	Relative activity (%)						
	WT	H301N	S19A	E26A	S300A	T294S	T294A
Phenyl acetate	100.0 ± 1.2	0.00	0.00	10.0 ± 2.6	70.3 ± 1.7	45.8 ± 3.5	58.9 ± 9.1
Butyl acetate	100.0 ± 0.6	0.00	0.00	0.00	30.1 ± 0.2	12.0 ± 0.9	21.4 ± 1.2
pNP-acetate	100.0 ± 0.6	0.00	0.00	8.6 ± 2.2	68.8 ± 0.3	42.9 ± 5.4	32.4 ± 0.3

The active site in SGNH hydrolases is a modification of the classical serine protease catalytic triad that contains serine, histidine, and aspartate, the latter participating in the charge relay system necessary for activation of the serine nucleophile. In SGNH enzymes, the serine and histidine are always present while the aspartate/glutamate is absent in some of these enzymes, for example, SsEst from *S. scabies*. In the latter case, a Group-I SGNH hydrolase, it was postulated that the role of an acidic sidechain is taken over by a mainchain carbonyl group.[42] The active site residues of SsEst are Ser14 and His283 and the carbonyl group is provided by the mainchain of Trp280. Superposition of the NanS structure with other SGNH hydrolases shows that the active site serine and histidine correspond to Ser19 and His301. However, NanS has neither an acidic sidechain nor a carbonyl group in the vicinity of His301. Instead, there are two polar residues that could potentially fulfill the role of the third member of the "classic" catalytic triad, Ser300 and Thr294. The first, Ser300, is an unlikely candidate as the $OG1^{Ser300}$ hydroxyl is ~3.9 Å from the $ND1^{His301}$ atom, and the hydroxyl group is nearly perpendicular to the imidazole ring of His300 when the latter forms a hydrogen bond to Ser 19. This $OG1^{Ser300}$ hydroxyl group forms a strong hydrogen bond to the mainchain carbonyl O^{Leu297} (2.6 Å) [Fig. 3(c)]. The other close neighbor of His301, Thr294, points its hydroxyl group OG1 toward the $ND1^{His301}$ atom (~3.9 Å) and is in an appropriate orientation to form a hydrogen bond. This Thr294 hydroxyl group makes a simultaneous hydrogen bond to $OE2^{Glu26}$ (2.8 Å) [Fig. 3(c)].

To confirm that Ser19 and His301 are indeed catalytically essential, these residues were mutated to Ala and Gln, respectively, and enzyme activity measured against phenyl, butyl, and pNP acetate, all of which showed significant activity with wild-type enzyme. In both cases, the mutants had no activity even though they behaved as well-folded, monomeric enzymes by gel filtration, dynamic light scattering, native gel, and CD analysis.

A further four mutants were tested to see if the third component of the catalytic triad could be identified. These mutants were S300A, T294A, T294S, and E26A. It was hypothesized that if T294A resulted in a decrease in activity, T294S may restore this activity. These four mutants were expressed in BL21(DE3)Star cells, and the proteins behaved similarly to the wild type during purification. All four mutants had the same CD spectra identical to the native protein (Supporting Information Fig. S1), indicating that they were all correctly folded. All mutants showed activity against three standard esterase substrates, although the level of activity was somewhat lower than the wild type enzyme [Fig. 1(b), Table II]. This shows that Thr294 is not essential for catalysis and leaves the question of the third member of the triad open. Most affected was the E26A mutant, which retained only ~10% wild type activity. Glu26 is 5.5Å from His301 and could not perform the classical function in catalysis. The carbonyl of Arg298, residue equivalent to Trp280 in SsEst, is also not close enough to His301 due to different conformations of the loop following the active site histidine in these enzymes. We hypothesize that either the catalytic role is played by a hydroxyl ion or a reorganization of the active site occurs upon substrate binding.

In summary, we have shown here that NanS is a sialate esterase that deacetylates the 9-*O'* position of sialic acid. The structure reveals that it is a member of the SGNH hydrolase family containing a catalytic Ser-His dyad. Based upon patterns of both sequence and structural conservation, we subdivided the SGNH family into two subfamilies. As yet, NanS has not been classified into a carbohydrate esterase family.

Materials and Methods

Cloning, expression, and purification

The *yjhS* gene from *E. coli* O157:H7 (Z5905) was PCR amplified and inserted into a modified pET15b vector (EMD Biosciences, San Diego, CA) to obtain a fusion protein containing a noncleavable N-terminal $(His)_6$ tag. Point mutations were introduced into *yjhS* using mutagenic primers. All mutations were confirmed by sequencing. For expression of unlabelled proteins, both the wild-type and genes containing S18A or H301N mutations were transformed into BL21(DE3) cells, while the mutant plasmids containing the E26A, T294A, T294S, and S300A mutants were transformed into BL21(DE3)Star cells. For preparation of SeMet-substituted protein, the *E.*

coli methionine auxotroph DL41 was transformed with the vector and protein expressed in 1 L LeMaster medium containing 100 μg mL^{-1} ampicillin.[45] Cells were grown for 2 h at 37°C, then induced with 100 μM IPTG and cultured at 21°C for 16 h. Cells were harvested by centrifugation (4000*g*, 30 min, 4°C), resuspended in 50 m*M* Tris-HCl pH 7.5, 400 m*M* NaCl, 1% (v/v) Triton X-100, 5% (v/v) glycerol, 10 m*M* β-mercaptoethanol, 20 m*M* imidazole and a cocktail of protease inhibitors (10 μM leupeptin (Boehringer Mannheim, Canada), 0.5 m*M* benzamidine (Sigma Aldrich), 0.1 m*M* Pefabloc™ (Roche)). Cell lysis was achieved by sonication for a total of 2 minutes with on and off cycles of 15 s duration and clarified by centrifugation (150,000*g*, 45 min, 4°C). The lysate supernatant was incubated with 1 mL Ni-NTA (Qiagen Inc., Canada) for 1 h with shaking. Beads were washed with 50 m*M* Tris-HCl pH 7.5, 1*M* NaCl, 5% (v/v) glycerol, 10 m*M* β-mercaptoethanol, 20 m*M* imidazole followed by the same buffer containing 0.4 *M* NaCl and 40 m*M* imidazole. The elution of the histidine-tagged protein was achieved with buffer containing 250 m*M* imidazole. Purified protein was concentrated by ultrafiltration to 22 mg mL^{-1} in the final buffer consisting of 20 m*M* Tris-HCl pH 7.5, 0.2*M* NaCl, 5 % (v/v) glycerol, 5 m*M* DTT. Mutant proteins were purified under similar conditions as for wild-type enzyme.

The total selenium incorporation as selenomethionine in the protein was confirmed by ESI-MS on an Agilent 1100 series mass spectrometer using an isocratic condition of 30% (v/v) acetonitrile containing 0.1% (v/v) formic acid. NanS mutants were also confirmed by ESI-MS. Dynamic light scattering measurements were performed for all samples using a DynaPro plate reader (Wyatt Technology Corporation, Santa Barbara, CA) at room temperature. Size exclusion chromatography using a Superdex 75 (10/16) column (Amersham Bioscience) on an ÄKTA purifier (Amersham Bioscience) was performed in the crystallization buffer to ascertain the oligomeric state of the purified protein. Circular Dichroism was carried out using a Jasco J-815 Spectrometer. Samples were dialyzed into 10 m*M* Potassium Phosphate pH 7.5, 20 m*M* NaF and were tested at a final concentration of 0.2 mg mL^{-1}.

Crystallization, data collection, and refinement

Initial crystallization conditions were identified using sparse matrix screens from Hampton Research (Hampton Research, Aliso Viejo, CA). The best diffracting crystals were obtained by mixing 1 μL protein in the final buffer with 1 μL of reservoir solution containing 0.2*M* NaCl, 0.1*M* Bis-Tris pH 5.5, 30% (w/v) PEG 3350, in micro batch experiments under oil. Prior to data collection crystals were flash frozen in the N$_2$ cold stream at 100 K (Oxford Cryosystem, Oxford, UK). SeMet crystals belong to space group $P2_12_12_1$ with unit cell dimensions $a = 41.1$ Å, $b = 131.9$ Å, $c = 172.2$ Å ($Z = 12$) and Mathews coefficient of 2.2 Å^{3}Da^{-1} with a solvent content of ∼42%. Native crystals were obtained from the same conditions. These crystals also belong to space group $P2_12_12_1$ but have different cell dimensions, $a = 41.1$ Å, $b = 57.9$ Å, $c = 135.4$ Å and contain one molecule in the asymmetric unit.

Data collection of the SeMet-labeled NanS crystals were carried out using a two wavelength MAD regime (peak, inflection point) to 2.2 Å resolution with a Quantum-4 CCD detector (Area Detector Systems Corp., San Diego, CA) at beamline X29, National Synchrotron Light Source, Brookhaven National Laboratory. Data processing and scaling were performed with HKL2000.[46] Of 18 expected selenium atoms in the asymmetric unit 15 were located with SHELXD[47] and refined further using SHARP[48] to obtain preliminary phases with a figure of merit of 0.43. Solvent flattening and iterative model building using the RESOLVE auto-build procedure [49] resulted in automated building of 92% of the overall model. The model was completed manually using XtalView[50] and Coot[51] and refined with REFMAC5[52] (Table III).

A native data set was collected to 1.6 Å resolution from a single crystal at the Canadian Light Source (CLS), Saskatoon, Saskatchewan. Data was processed and scaled using HKL2000.[46] The SeMet model was used to solve the native data set by molecular replacement using Phaser[53] and refined with REFMAC5 to a final R_{work} of 0.201 and R_{free} of 0.242. The final model of NanS contains residues 4-325 with one short regions, 216–18, lacking clearly defined electron density. The model has good stereochemistry as analyzed using Molprobity.[54]

Determination of enzyme activity

To determine the substrate profile of NanS, assays with various carboxyl esters were carried out according to the published protocol.[37] The reaction mixture in a final volume of 105 μL contained 3 to 30 μg mL^{-1} of enzyme in 4.5 m*M* *N*,*N*-bis(2-hydroxyethyl)-2-aminoethanesulfonic acid (BES) buffer pH 7.2, 0.44 m*M* indicator 4-nitrophenol (pNP) and 1 m*M* of substrate. The high buffer concentration related to pNP is critical to sense small changes in pH with minor modifications in the reaction conditions. The reaction was initiated by the addition of enzyme and the color change of the indicator dye was continuously monitored for 10 min at 412 nm at 25°C. Activity was estimated from the linear range of the reaction, with the typical variation of OD$_{412}$ in a range of 5 to 50 mAU. The 9-*O*-acetyl sialic acid used as substrates in the screening panel was a gift from Dr. Shawn DeFrees (Neose Technologies, Horsham, PA). 9-*O*-acetyl-GD3-*S*-phenyl was synthesized by adding enzymatically the *O*-acetyl group to

Table III. *X-ray Crystallographic Data*

Dataset	Se-Met (Peak)	Apo
	Data collection	
Space Group	$P2_12_12_1$	$P2_12_12_1$
	Unit Cell	
a,b,c (Å)	41.1, 131.9, 172.2	41.1, 57.9, 135.4
Resolution (Å)	50.0–2.2	38.8–1.6
Z[a]	12	4
Resolution (Å)	50–2.2 (2.28-2.20)	33.8–1.6 (1.66–1.6)
Wavelength (Å)	0.9793	0.9793
Unique hkl	84455[b]	40213[b]
Redundancy	3.2 (2.7)	7.2 (7.3)
Completeness	92.0 (79.0)	92.8 (100)
R_{sym}[c]	0.053 (0.222)	0.097 (0.430)
$I/\sigma(I)$	16.2 (4.9)	27 (5.2)
	Refinement	
R_{work}[d] (# hkl)		0.201
R_{free}[d] (# hkl)		0.242
Average B-factors		
Protein		15
Solvent		26
Ramachandran plot		
Allowed (%)		96.9
Generous (%)		3.1
Disallowed (%)		0.0
rms bonds (Å)		0.012
rms angles (°)		1.43
PDB code		3PT5

[a] Number of molecules in the unit cell.
[b] Bijovet pairs unmerged.
[c] $R_{sym} = (\Sigma |I_{obs} - I_{avg}|)/\Sigma I_{avg.}$
[d] $R_{work/free} = (\Sigma |F_{obs} - F_{calc}|)/\Sigma F_{obs.}$

the terminal NeuAc in GD3-*S*-phenyl (NeuAcα-2,8-NeuAcα-2,3-Galβ-1,4-Glcβ-*S*-phenyl) using a recombinant sialic acid *O*-acetyltransferase from *Campylobacter jejuni*.[55] Aryl esterase activity was measured by continuous monitoring at 310 nm for 2–3 min using 2.6 µg mL⁻¹ enzyme in 50 m*M* BES pH 7.2, at a substrate concentration of 1 m*M*. The substrates used were, α-naphthyl acetate, β-naphthyl acetate, α-naphthyl-propionate, α-naphthyl-propionate, α-naphthyl dodecanoate. NanS was also screened for lipolytic using Tween 80 as enzyme substrate[56] as well as thioesterase[57] activities. The thioester substrates used were DL-3-hydroxy-3-methylglutaryl-CoA, methylmalonyl-CoA, phenylacetyl-CoA, phenylacetyl-CoA, hexanoyl-CoA, succinyl-CoA, stearoyl-CoA, octanoyl-CoA, hydroxybutyryl-CoA, palmitoyl-CoA, methyl-crotonyl-CoA, glutaryl-CoA, acetyl-CoA, dodecanoyl-CoA, malonyl-CoA.

To determine the residual activity of the NanS mutant proteins, enzymatic activity was monitored on the butyl acetate and phenyl acetate substrates previously identified to be preferential substrates of the wild type protein. The reaction mixture contained 30 µg mL⁻¹ of enzyme in 4.5 m*M* BES buffer pH 7.2, 0.44 m*M* indicator 4-nitrophenol and 1 m*M* of substrate. The reaction was initiated by the addi-

tion of enzyme and the color change of the indicator dye was monitored for 10 min at 412 nm at 25°C. Additionally, residual activity of NanS mutants was monitored by following the hydrolysis of pNP-acetate. The final reaction mixture contained 20 m*M* Tris pH 7.5, 1 m*M* pNP-acetate substrate, and 3 µg mL⁻¹ NanS. The reaction was monitored at 412 nm for 10 min at 25°C. Samples were monitored in triplicate, and data are expressed as percentage residual activity in comparison with the native NanS protein.

References

1. Cantarel BL, Coutinho PM, Rancurel C, Bernard T, Lombard V, Henrissat B (2009) The Carbohydrate-Active EnZymes database (CAZy): an expert resource for Glycogenomics. Nucleic Acids Res 37:D233–D238.
2. Williamson G (1991) Purification and characterization of pectin acetylesterase from orange peel. Phytochemistry 30:445–449.
3. Sundberg M, Poutanen K (1991) Purification and properties of two acetylxylan esterases of Trichoderma reesei. Biotech Appl Biochem 13:1–11.
4. Tenkanen M, Thornton J, Viikari L (1995) An acetyl-glucomannan esterase of Aspergillus oryzae; purification, characterization and role in the hydrolysis of O-acetyl-galactoglucomannan. J Biotechnol 42:197–206.
5. Araki Y, Ito E (1974) A pathway of chitosan formation in Mucor rouxii: enzymatic deacetylation of chitin. Biochem Biophys Res Commun 56:669–675.
6. Navarro-Fernandez J, Martinez-Martinez I, Montoro-Garcia S, Garcia-Carmona F, Takami H, Sanchez-Ferrer A (2008) Characterization of a new rhamnogalacturonan acetyl esterase from Bacillus halodurans C-125 with a new putative carbohydrate binding domain. J Bacteriol 190:1375–1382.
7. Corfield AP, Wagner SA, Clamp JR, Kriaris MS, Hoskins LC (1992) Mucin degradation in the human colon: production of sialidase, sialate O-acetylesterase, N-acetylneuraminate lyase, arylesterase, and glycosulfatase activities by strains of fecal bacteria. Infect Immun 60:3971–3978.
8. Steenbergen SM, Jirik JL, Vimr ER (2009) YjhS (NanS) is required for Escherichia coli to grow on 9-O-acetylated N-acetylneuraminic acid. J Bacteriol 191:7134–7139.
9. Vimr ER, Steenbergen SM (2006) Mobile contingency locus controlling Escherichia coli K1 polysialic acid capsule acetylation. Mol Microbiol 60:828–837.
10. Blair DE, Hekmat O, Schüttelkopf AW, Shrestha B, Tokuyasu K, Withers SG, van Aalten DMF (2006)

Structure and mechanism of chitin deacetylase from the fungal pathogen Colletotrichum lindemuthianum. Biochemistry 45:9416–9426.

11. Weadge JT, Clarke AJ (2006) Identification and characterization of O-acetylpeptidoglycan esterase: a novel enzyme discovered in Neisseria gonorrhoeae. Biochemistry 45:839–851.

12. Caufrier F, Martinou A, Dupont C, Bouriotis V (2003) Carbohydrate esterase family 4 enzymes: substrate specificity. Carbohydr Res 338:687–692.

13. Deli A, Koutsioulis D, Fadouloglou VE, Spiliotopoulou P, Balomenou S, Arnaouteli S, Tzanodaskalaki M, Mavromatis K, Kokkinidis M, Bouriotis V (2010) LmbE proteins from Bacillus-cereus are de-N-acetylases with broad substrate specificity and are highly similar to proteins in Bacillus-anthracis. FEBS J 277:2740–2753.

14. Degrassi G, Kojic M, Ljubijankic G, Venturi V (2000) The acetyl xylan esterase of Bacillus pumilus belongs to a family of esterases with broad substrate specificity. Microbiology 146:1585–1591.

15. Topakas E, Kyriakopoulos S, Biely P, Hirsch J, Vafiadi C, Christakopoulos P (2010) Carbohydrate esterases of family 2 are 6-O-deacetylases. FEBS Lett 584:543–548.

16. Vimr E, Lichtensteiger C (2002) To sialylate, or not to sialylate: that is the question. Trends Microbiol 10:254–257.

17. Fujimoto I, Bruses JL, Rutishauser U (2001) Regulation of cell adhesion by polysialic acid. J Biol Chem 276:31745–31751.

18. Almagro-Moreno S, Boyd EF (2009) Insights into the evolution of sialic acid catabolism among bacteria. BMC Evol Biol 9:118.

19. Kalivoda KA, Steenbergen SM, Vimr ER, Plumbridge J (2003) Regulation of sialic acid catabolism by the DNA binding protein NanR in Escherichia coli. J Bacteriol 185:4806–4815.

20. Condemine G, Berrier C, Plumbridge J, Ghazi A (2005) Function and expression of an N-acetylneuraminic acid-inducible outer membrane channel in Escherichia coli. J Bacteriol 187:1959–1965.

21. Severi E, Muller A, Potts JR, Leech A, Williamson D, Wilson KS, Thomas GH (2008) Sialic acid mutarotation is catalyzed by the Escherichia coli beta-propeller protein YjhT. J Biol Chem 283:4841–4849.

22. Lewis AL, Cao H, Patel SK, Diaz S, Ryan W, Carlin AF, Thon V, Lewis WG, Varki A, Chen X, Nizet V (2007) NeuA sialic acid O-acetylesterase activity modulates O-acetylation of capsular polysaccharide in Group B Streptococcus. J Biol Chem 282:27562–27571.

23. Steenbergen SM, Lee YC, Vann WF, Vionnet J, Wright LF, Vimr ER (2006) Separate pathways for O acetylation of polymeric and monomeric sialic acids and identification of sialyl O-acetyl esterase in Escherichia coli K1. J Bacteriol 188:6195–6206.

24. Stoddart A, Zhang Y, Paige CJ (1996) Molecular cloning of the cDNA encoding a murine sialic acid-specific 9-O-acetylesterase and RNA expression in cells of hematopoietic and non-hematopoietic origin. Nucleic Acids Res 24:4003–4008.

25. Pillai S, Cariappa A, Pirnie SP (2009) Esterases and autoimmunity: the sialic acid acetylesterase pathway and the regulation of peripheral B cell tolerance. Trends Immunol 30:488–493.

26. Surolia I, Pirnie SP, Chellappa V, Taylor KN, Cariappa A, Moya J, Liu H, Bell DW, Driscoll DR, Diederichs S, Haider K, Netravali I, Le S, Elia R, Dow E, Lee A, Freudenberg J, De Jager PL, Chretien Y, Varki A, Macdonald ME, Gillis T, Behrens TW, Bloch D, Collier D, Korzenik J, Podolsky DK, Hafler D, Murali M, Sands B, Stone JH, Gregersen PK, Pillai S (2010) Functionally defective germline variants of sialic acid acetylesterase in autoimmunity. Nature 466:243–247.

27. Herrler G, Rott R, Klenk HD, Muller HP, Shukla AK, Schauer R (1985) The receptor-destroying enzyme of influenza C virus is neuraminate-O-acetylesterase. EMBO J 4:1503–1506.

28. Smits SL, Gerwig GJ, van Vliet ALW, Lissenberg A, Briza P, Kamerling JP, Vlasak R, de Groot RJ (2005) Nidovirus sialate-O-acetylesterases. J Biol Chem 280:6933–6941.

29. Molgaard A, Kauppinen S, Larsen S (2000) Rhamnogalacturonan acetylesterase elucidates the structure and function of a new family of hydrolases. Structure 8:373–383.

30. Ollis DL, Cheah E, Cygler M, Dijkstra BW, Frolow F, Franken SM, Harel M, Remington SJ, Silman I, Schrag JD, Sussman JL, Verscheuren KHG, Goldman A (1992) The alpha/beta hydrolase fold. Protein Eng 5:197–211.

31. Lo YC, Lin SC, Shaw JF, Liaw YC (2003) Crystal structure of Escherichia coli thioesterase I/protease I/lysophospholipase L1: consensus sequence blocks constitute the catalytic center of SGNH-hydrolases through a conserved hydrogen bond network. J Mol Biol 330:539–551.

32. Blair DE, Schüttelkopf AW, MacRae JI, van Aalten DMF (2005) Structure and metal-dependent mechanism of peptidoglycan deacetylase, a streptococcal virulence factor. Proc Natl Acad Sci USA 102:15429–15434.

33. Blair DE, van Aalten DMF (2004) Structures of Bacillus subtilis PdaA, a family 4 carbohydrate esterase, and a complex with N-acetyl-glucosamine. FEBS Lett 570:13–19.

34. Vincent F, Charnock SJ, Verschueren KHG, Turkenburg JP, Scott DJ, Offen WA, Roberts S, Pell G, Gilbert HJ, Davies GJ, Brannigan JA (2003) Multifunctional xylooligosaccharide/cephalosporin C deacetylase revealed by the hexameric structure of the Bacillus subtilis enzyme at 1.9 Å resolution. J Mol Biol 330:593–606.

35. Burland V, Plunkett G, Sofia HJ, Daniels DL, Blattner FR (1995) Analysis of the Escherichia coli genome VI: DNA sequence of the region from 92.8 through 100 minutes. Nucleic Acids Res 23:2105–2119.

36. Robbe-Masselot C, Maes E, Rousset M, Michalski JC, Capon C (2009) Glycosylation of human fetal mucins: a similar repertoire of O-glycans along the intestinal tract. Glycoconj J 26:397–413.

37. Janes LE, Löwendahl AC, Kazlauskas RJ (1998) Quantitative screening of hydrolase libraries using pH indicators: identifying active and enantioselective hydrolases. Chem Eur J 4:2324–2331.

38. Kuznetsova E, Proudfoot M, Sanders SA, Reinking J, Savchenko A, Arrowsmith CH, Edwards AM, Yakunin AF (2005) Enzyme genomics: application of general enzymatic screens to discover new enzymes. FEMS Microbiol Rev 29:263–279.

39. Holm L, Sander C (1995) Dali: a network tool for protein structure comparison. Trends Biochem Sci 20:478–480.

40. Bitto E, Bingman CA, Allard ST, Wesenberg GE, Phillips GN,Jr. (2005) The structure at 1.7 A resolution of the protein product of the At2g17340 gene from Arabidopsis thaliana. Acta Cryst F61:630–635.

41. Mathews I, Soltis M, Saldajeno M, Ganshaw G, Sala R, Weyler W, Cervin MA, Whited G, Bott R (2007) Structure of a novel enzyme that catalyzes acyl transfer to alcohols in aqueous conditions. Biochemistry 46:8969–8979.

42. Wei Y, Schottel JL, Derewenda U, Swenson L, Patkar S, Derewenda ZS (1995) A novel variant of the catalytic triad in the Streptomyces scabies esterase. Nat Struct Biol 2:218–223.

43. Ho YS, Swenson L, Derewenda U, Serre L, Wei Y, Dauter Z, Hattori M, Adachi T, Aoki J, Arai H, Inoue K, Derewenda ZS (1997) Brain acetylhydrolase that inactivates platelet-activating factor is a G-protein-like trimer. Nature 385:89–93.

44. Rosenthal PB, Zhang X, Formanowski F, Fitz W, Wong CH, Meier-Ewert H, Skehel JJ, Wiley DC (1998) Structure of the haemagglutinin-esterase-fusion glycoprotein of influenza C virus. Nature 396:92–96.

45. Hendrickson WA, Horton JR, LeMaster DM (1990) Selenomethionyl proteins produced for analysis by multiwavelength anomalous diffraction (MAD): a vehicle for direct determination of three-dimensional structure. EMBO J 9:1665–1672.

46. Otwinowski Z, Minor W (1997) Processing of X-ray diffraction data collected in oscillation mode. Methods Enzymol 276:307–326.

47. Schneider TR, Sheldrick GM (2002) Substructure solution with SHELXD. Acta Cryst D58:1772–1779.

48. Bricogne G, Vonrhein C, Flensburg C, Schiltz M, Paciorek W (2003) Generation, representation and flow of phase information in structure determination: recent developments in and around SHARP 2.0. Acta Cryst D59:2023–2030.

49. Terwilliger TC (2000) Maximum-likelihood density modification. Acta Cryst D56:965–972.

50. McRee DE (1999) XtalView/Xfit—a versatile program for manipulating atomic coordinates and electron density. J Struct Biol 125:156–165.

51. Emsley P, Cowtan K (2004) Coot: model-building tools for molecular graphics. Acta Cryst D 60:2126–2132.

52. Murshudov GN, Vagin AA, Dodson EJ (1997) Refinement of macromolecular structures by the maximum-likelihood method. Acta Cryst D 53:240–255.

53. McCoy AJ, Grosse-Kunstleve RW, Adams PD, Winn MD, Storoni LC, Read RJ (2007) Phaser crystallographic software. J Appl Cryst 40:658–674.

54. Chen VB, Arendall III WB, Headd JJ, Keedy DA, Immormino RM, Kapral GJ, Murray LW, Richardson JS, Richardson C (2010) MolProbity: all-atom structure validation for macromolecular crystallography. Acta Cryst D 66:12–21.

55. Houliston RS, Endtz HP, Yuki N, Li J, Jarrell HC, Koga M, van BA, Karwaski MF, Wakarchuk WW, Gilbert M (2006) Identification of a sialate O-acetyltransferase from Campylobacter jejuni: demonstration of direct transfer to the C-9 position of terminalalpha-2, 8-linked sialic acid. J Biol Chem 281:11480–11486.

56. von Tigerstrom RG, Stelmaschuk S (1989) The use of Tween 20 in a sensitive turbidimetric assay of lipolytic enzymes. Can J Microbiol 35:511–514.

57. Berge RK, Aarsland A, Bakke OM, Farstad M (1983) Hepatic enzymes, CoASH and long-chain acyl-CoA in subcellular fractions as affected by drugs inducing peroxisomes and smooth endoplasmic reticulum. Int J Biochem 15:191–204.